

RESEARCH ARTICLE

Solamargine inhibits the growth of hepatocellular carcinoma and enhances the anticancer effect of sorafenib by regulating HOTTIP-TUG1/miR-4726-5p/MUC1 pathway

Qing Tang^{1,2,3}  | Xiaojuan Li⁴ | Yun Chen⁵ | Shunqin Long^{1,2,3} | Yaya Yu⁶ | Honghao Sheng^{1,2,3} | Sumei Wang^{1,2,3} | Ling Han^{2,7,8} | Wanyin Wu^{1,2,3}

¹Department of Oncology, Clinical and Basic Research Team of TCM Prevention and Treatment of NSCLC, The Second Clinical College of Guangzhou University of Chinese Medicine, Guangdong Provincial Hospital of Chinese Medicine, Guangzhou, Guangdong, P.R. China

²Guangdong Provincial Key Laboratory of Clinical Research on Traditional Chinese Medicine Syndrome, Guangzhou, Guangdong, P.R. China

³Guangdong-Hong Kong-Macau Joint Lab on Chinese Medicine and Immune Disease Research, Guangzhou University of Chinese Medicine, Guangzhou, Guangdong, P.R. China

⁴Shanghai University of Traditional Chinese Medicine, Shanghai, P.R. China

⁵Department of Organ Transplantation, Second Affiliated Hospital of Guangzhou Medical University, Guangzhou, Guangdong, P.R. China

⁶Department of Oncology, The Second Affiliated Hospital of Guangzhou University of Chinese Medicine, Guangdong Provincial Hospital of Chinese Medicine, Guangzhou, Guangdong, P.R. China

⁷The Second Clinical College of Guangzhou University of Chinese Medicine, Guangdong Provincial Hospital of Chinese Medicine, Guangzhou, Guangdong, P.R. China

⁸Guangdong Provincial Academy of Chinese Medical Sciences, Guangzhou, Guangdong, P.R. China

Correspondence

Sumei Wang, Ling Han, and Wanyin Wu, The Second Clinical Medical College of Guangzhou University of Chinese Medicine, 111 Dade Rd., Guangzhou, Guangdong 510120, P.R. China. Email: wangsume198708@163.com, linghan36@163.com, and wwanyin@126.com

Funding information

Chinese medicine science and technology research project of Guangdong Provincial Hospital of Chinese Medicine (YN2019MJ09, YN2019QJ06); Natural Science Foundation of China (81871863); State key laboratory of Dampness Syndrome of Chinese Medicine Special Fund (SZ2021ZZ29); Scientific Research Project in Universities of Guangdong Provincial Department of Education (2020KTSCX029); Guangdong Provincial Key Laboratory of Clinical Research on Traditional Chinese Medicine Syndrome (ZH2020KF03); postgraduate research innovation project of

Abstract

Hepatocellular carcinoma (HCC) is one of the most common primary malignancies. Drug resistance has significantly prevented the clinical application of sorafenib (SF), a first-line targeted medicine for the treatment of HCC. Solamargine (SM), a natural alkaloid, has shown potential antitumor activity, but studies about antitumor effect of SM are obviously insufficient in HCC. In the present study, we found that SM significantly inhibited the growth of HCC and enhanced the anticancer effect of SF. In brief, SM significantly inhibited the growth of HepG2 and Huh-7 cells. The combination of SM and SF showed a synergistic antitumor effect. Mechanistically, SM downregulated the expression of long noncoding RNA HOTTIP and TUG1, followed by increasing the expression of miR-4726-5p. Moreover, miR-4726-5p directly bound to the 3'-UTR region of MUC1 and decreased the expression of MUC1 protein. Overexpression of MUC1 partially reversed the inhibitory effect of SM on HepG2 and Huh-7 cells viability, which suggested that MUC1 may be the key target in SM-induced growth inhibition of HCC. More importantly, the combination

Abbreviations: HCC, hepatocellular carcinoma; HOTTIP, HOXA distal transcript antisense RNA; MUC1, mucin 1; SF, sorafenib; SM, solamargine; TUG1, taurine upregulated 1.

Qing Tang, Xiaojuan Li, and Yun Chen contributed equally to this study.

This is an open access article under the terms of the Creative Commons Attribution-NonCommercial-NoDerivs License, which permits use and distribution in any medium, provided the original work is properly cited, the use is non-commercial and no modifications or adaptations are made.

© 2022 The Authors. *Molecular Carcinogenesis* published by Wiley Periodicals LLC

Guangzhou University of Chinese Medicine
(A1-2606-21-429-001Z53)

of SM and SF synergistically restrained the expression of MUC1 protein. Taken together, our study revealed that SM inhibited the growth of HCC and enhanced the anticancer effect of SF through HOTTIP-TUG1/miR-4726-5p/MUC1 signaling pathway. These findings will provide potential therapeutic targets and strategies for the treatment of HCC.

KEYWORDS

hepatocellular carcinoma, MUC1, solamargine, sorafenib, synergistic anticancer effect

1 | INTRODUCTION

Hepatocellular carcinoma (HCC) is the most common primary malignancy with poor prognosis and the third leading cause of cancer-related death worldwide. Over the past few decades, the incidence of HCC and HCC-related death has continued to rise. However, the treatment strategies for advanced HCC are very limited.¹⁻³ Therefore, continuing efforts have been made to select more effective therapies to intervene in this malignancy to improve quality of life and prolong survival.

Solamargine (SM), a natural sugar alkaloid extracted from the fruits of Solanaceae plants, has been fully confirmed by our previous studies and other reports that SM can significantly inhibit the occurrence and development of a variety of cancers.⁴⁻⁷ The growing number of studies have found that SM exhibits its antitumor activity through multifarious pathways, including tumor growth pathways, apoptosis-related pathways, mitochondrial pathways, protein kinase pathways, and so on.⁸ For example, SM significantly suppresses the expression of X-linked apoptosis inhibitor, PCNA, and cyclin D1, while increasing the activity of caspase-3 to induce apoptosis. Moreover, SM inhibits the metastasis of tumor cells by regulating the expression of matrix metalloproteinase.⁹ However, the role of SM in the growth of HCC is rarely studied, and the molecular mechanism needs to be further clarified. In this study, we revealed that SM significantly inhibited the cell growth and proliferation in HCC by regulating the interaction between long noncoding RNAs (lncRNAs) and microRNAs (miRNAs), which suggested a novel mechanism for SM-induced inhibition of HCC.

LncRNA generally refers to the transcriptional products with a length of more than 200 nucleotides, which is called noncoding RNA and does not translate proteins. LncRNA is abnormally expressed in various types of cancer and plays an important role in the occurrence and development of cancer.¹⁰ HOTTIP, a lncRNA encoded in the 5-terminus genomic region of the HoxA site, is made up of 3764 nucleotides. Abnormal expression of HOTTIP is involved in the progression of almost all types of human cancer, including proliferation, invasion, and migration of cancer cells.¹¹ While TUG1, another lncRNA, locates on chromosome 22q12.2 and contains 7598 nucleotides. TUG1 plays an important role in the biological processes of a variety of cancers, and increased TUG1 expression is closely related to poor prognosis, tumor size, pathological stage, and distant

metastasis of cancers.^{12,13} In addition to being associated with other cancers, HOTTIP and TUG1 are also closely related to HCC. For example, miR-122 and miR-204 might inhibit the HCC progress by downregulation of HOTTIP expression.¹⁴ In addition, HOTTIP might be a potential therapeutic target, the high expression level of HOTTIP in HCC could serve as a candidate biomarker for predicting poor prognosis in HCC patients.¹⁵ On the other hand, TUG1 could promote the proliferation, migration, and invasion of HCC through regulating the miR-29C-3p/COL1A1 axis.¹⁶ Moreover, TUG1 is associated with the serum alpha-fetoprotein level and the pathogenesis of HCC.¹⁷⁻¹⁹ Therefore, the role of HOTTIP and TUG1 in HCC has aroused our interest, it is extremely important to study their role in HCC.

Similarly, miRNAs have gradually become a focus of tumor research and play a key role in tumorigenesis by regulating various aspects of tumors, including cell cycle, metastasis, angiogenesis, metabolism, and apoptosis pathways.²⁰ Among these miRNAs, miR-4726-5p has been reported to be associated with growth and progression in cancers. For example, miR-4726-5p may involve in the tumorigenesis of laryngeal squamous cell carcinoma.²¹ MiR-4726-5p is also correlated with anthracycline cardiotoxicity in breast cancer patients.²² Apart from that, miR-4726-5p may mediate the function of hematopoietic stem cells and the process of intervertebral disc degeneration.^{23,24} However, miR-4726-5p has been still rarely studied in human cancer. In our study, miR-4726-5p was found to mediate the growth inhibition of SM on HCC cells. SM significantly increased the expression of miR-4726-5p, which directly targets MUC1 and downregulated MUC1 protein expression, finally suppressed the cell growth and proliferation of HCC. However, the role of miR-4726-5p in the progression of HCC needs to be further investigated.

More importantly, recent studies have shown that MUC1 is a class of mucins highly expressed in tumor cells, which can destroy intercellular adhesion and immune response, change intracellular signal transduction pathway and induce tumor metastasis, but its prognostic significance in HCC is still controversial.^{25,26} In our study, miR-4726-5p may act as a sponge for MUC1 and regulate its expression. However, it is important to note that only limited studies have demonstrated an association between HOTTIP, TUG1, miR-4726-5p, and MUC1. Therefore, there is still a gap in understanding the role of this interaction in HCC.

2 | MATERIALS AND METHODS

2.1 | Cell culture and reagents

Antibodies for MUC1 and GAPDH were obtained from Cell Signaling Technology Inc. MiR-4726-5p mimics were obtained from RiboBio Co., Ltd. MiR-4726-5p and U6 primers were purchased from GenePharma. HOTTIP, TUG1, and GAPDH primers were purchased from Life Technologies. Lipofectamine 3000 reagent and RPMI 1640 cell culture medium were provided by Life Technologies. SM was obtained from Must Bio-technology Company. HepG2 and Huh-7 cells were purchased from Guangzhou Cellcook Biotech Co., Ltd. and authenticated for the absence of mycoplasma. Cells were cultured in RPMI 1640 medium supplemented with 10% fetal bovine serum at 37°C in a humidified atmosphere containing 5% CO₂. HepG2-Luc cells were constructed by Guangzhou Land Technology Co., Ltd. and cultured in a medium containing geneticin Sulfate (obtained from Life Technologies). Cells at 70% confluence were trypsinized with 0.25% trypsin and used in all in vitro experiments.

2.2 | Cell viability assay

The 3-(4,5-dimethylthiazol-2-yl)-2,5-diphenyltetrazolium bromide (MTT) assay was performed to detect the cell viability as described previously.⁴ HCC cells (about 4×10^3 cells/well) were seeded into 96-well plates and cultured overnight in an incubator with 5% CO₂ and 37°C. Cells were treated with indicated doses of SM for 24, 48, and 72 h, respectively, as well as treated with combination of SM and sorafenib (SF). Then plates were incubated with MTT solution (5 mg/ml) at 37°C for 4 h followed by adding dimethyl sulfoxide and shaking on an oscillator for 5 min. Microplate reader (Perkin Elmer, Victor X5) was used to measure absorbance at 570 nm. Cell viability was calculated as the ratio of absorbance of sample/control.

2.3 | EDU assay

Cell proliferation was measured by Cell-Light EDU Apollo 488 In Vitro Imaging Kit (RiboBio) according to instructions from the manufacturer. First of all, HepG2 and Huh-7 cells in 96-well plates were treated with SM for 24 h, then incubated with EDU reagent for 2 h and fixed in 4% paraformaldehyde for 30 min. After washing by glycine, cells were incubated in 0.2% Trion X-100 for 10 min followed by adding 1× Apollo reaction buffer, and then cells were stained with Hoechst (5 mg/ml). Microscope (BX53 + DP72, Olympus Corporation) was used to take images which were evaluated by an image analysis software (Media Cybernetics, Inc.). Percent cell proliferation was calculated as: (EDU positive cells/Hoechst stained cells) × 100.

2.4 | Western blot analysis

Western blot was performed as described previously.⁴ Equivalent proteins from whole-cell lysates mixed with 5× loading bufer were injected into 10% sodium dodecyl sulfate polyacrylamide gel for about 1.5 h of electrophoresis. The proteins were then transferred to PVDF membranes (Milipore). The PVDF membrane was incubated with antibodies against MUC1 (1:1000) and GAPDH (1:10,000) after being sealed with 5% skim milk powder for 1 h. The PVDF membrane was incubated with a horseradish peroxidase binding secondary antibody (1:3000; cellular signaling) for 1 h followed by washing three times with tris buffered saline tween and then transferred to the newly prepared ECL solution (Milipore). The signals were captured using a gel imaging system (Bio-Rad).

2.5 | Real-time quantitative PCR (qRT-PCR)

qRT-PCR was performed to detect the expression of HOTTIP, TUG1, and miR-4726-5p. Total RNA (1 µg) was reverted to complementary deoxyribonucleic acid (cDNA) using an oligonucleotide dT primer and a reverse transcriptase (Invitrogen) according to the instructions. A total of 20 µl of 2 µl cDNA and enzyme mixture was added to the polymerase chain reaction (PCR) tube for quantitative real-time PCR reaction in the PCR apparatus (Grand Island Applied Biological Systems). The PCR conditions were as follows: 30 s at 95°C, then 40 5 s at 95°C, 34 s at 60°C. Finally, the cycle is performed for 15 s at 95°C, 60 s at 60°C, and 95°C. Determine the threshold, mean error, and standard error for each sample/primer pair were calculated. Relative expression of HOTTIP, TUG1, miR-4726-5p, and MUC1 were calculated by using $2^{-\Delta\Delta Ct}$ equation. Primers were designed as follows:

HOTTIP forward: 5'-TCACAGAGAGTGGAAAC-3',
 HOTTIP reverse: 5'-CCCAGGATCCTCTCCCAT-3';
 TUG1 forward: 5-ACGACTGAGCAAGCACTACC-3',
 TUG1 reverse: 5-CTCAGCAATCAGGAGGCACA-3';
 MiR-4726-5p forward: 5-TCAGGGCCAGAGGAGCC -3',
 MiR-4726-5p reverse: 5- TATGGTTCTTCACGACTGGTTCAC-3';
 MUC1 forward: 5'-ACGTCAGCGTGAGTGATGTG-3',
 MUC1 reverse: 5'-GACAGACAGCCAAGGCAATG-3';
 U6 forward: 5'-ATTGGAACGATACAGAGAAGATT-3',
 U6 reverse: 5'-GGAACGCTTCACGAATTTG-3';
 GAPDH forward: 5'-CTCCTCCTGTTTCGACAGTCAGC-3',
 GAPDH reverse: 5'-CCCAATACGACCAAATCCGTT-3'.

2.6 | RNA fluorescence in situ hybridization (FISH) assay

RNA FISH was performed for the detection of miR-4726-5p situ expression in cells. HepG2 and Huh-7 cells were inoculated in 48-well plates (wells were pretreated with appropriate size coverslips) at

a density of 1.0×10^4 cells/well, mixed and incubated overnight at 37°C in a 5% CO₂ incubator. The next day, cells were treated with SM for 24 h. After washing the cells with PBS, 100 µl of 4% paraformaldehyde was added to each well and fixed at room temperature for 15 min. Four percentage of paraformaldehyde was discarded and the cells were treated with 70%, 85%, and anhydrous ethanol for 3 min, respectively according to the instructions. The probes were diluted to the appropriate concentration, then 100 µl of probe mixture was added to each well, followed by denaturing at 73°C for 5 min and incubating at 37°C for 12–16 h in an incubator. The cell nuclei were stained with 4',6-diamidino-2-phenylindole for 20 min with light avoidance and observed under a fluorescent microscope as soon as possible.

2.7 | Dual-luciferase reporter assay

The binding sites of MUC1, HOTTIP, and TUG1 for miR-4726-5p were predicted using bioinformatics prediction databases (TargetScan, MiRWalk, and MiRBase). The 3'-UTR cDNA fragment of MUC1 containing the wild-type and mutated miR-4726-5p binding sites (pEZXM-T05-Luc-MUC1-WT or pEZXM-T05-Luc-MUC1-Mut), and the cDNA fragments of HOTTIP (or TUG1) containing the wild-type and mutated miR-4726-5p binding sites (pEZXM-T05-Luc-HOTTIP [or TUG1]-WT or pEZXM-T05-Luc-HOTTIP [or TUG1]-Mut) were constructed by GeneCopoeia, Inc. Plasmids (1 g/ml medium) were transfected into cells using liposome 3000 reagent for 24 h and then treated with miR-4726-5p mimics for an additional 24 h. The secreted Pair Dual Luminescence Assay Kit (GeneCopoeia, Inc.) was used to prepare cell extracts and measure the cell luciferase activities which were normalized with secreted alkaline phosphatase activity within each sample.

2.8 | RNA immunoprecipitation (RIP) assay

RIP assay was performed using the Magna RIP RNA-Binding Protein Immunoprecipitation Kit (Millipore) following instruction from the manufacturer. Briefly, cells were collected in centrifuge tubes and incubated on ice for 5 min with an equal volume of complete RIP lysis buffer. RIP buffer was then added to each centrifuge tube. The cells lysates were incubated with magnetic beads coated with the specific PDPK1 antibody (Abcam), anti-Ago2 antibody (Millipore), or the negative control (NC) Immunoglobulin G (IgG) (Millipore) and all centrifuge tubes are placed on a spinner and incubated overnight at 4°C. The final volume of the immunoprecipitation reaction is 1.0 ml. Ten microliters of RIP supernatant lysate are placed at -80°C and marked as "input." The beads were washed six times with 0.5 ml of RIP wash buffer, and 50 µl of bead suspension was used for protein blotting assay to detect the immunoprecipitation efficiency. The washed precipitates and input samples were resuspended using proteinase K buffer. Finally, RNA was extracted and the expression of HOTTIP, TUG1, and miR-4726-5p were measured by qRT-PCR analysis.

2.9 | Transient transfection assays

Cells were seeded in 6-well or 96-well culture plates. MUC1 overexpression vectors (pCMV6-MUC1) or NC, and HOTTIP small interfering RNA (siRNA), TUG1 siRNA, or control siRNA (RiboBio Co.) were transfected by using Lipofectamine 3000 reagent before cells were grown to 60% confluency. Moreover, miR-4726-5p mimics were transfected with RiboFect CP reagent (RiboBio) according to the manufacturer's instructions. Briefly, Lipofectamine 3000 and siRNA or overexpressed plasmids were incubated in Opti-MEM medium (Invitrogen) for 5 min, respectively, then they were mixed gently, the mixture was incubated at room temperature for 15 min, and then added into the cell culture medium. The miRNA mimics were incubated with RiboFect CP Reagent, and then added into the cell culture medium. The cells were transfected for 24–72 h according to experimental needs.

2.10 | Immunohistochemistry (IHC) analysis

IHC was performed to determine the expression of MUC1 protein. Briefly, the xenografted tumors were fixed with 4% formaldehyde for 24 h before paraffin-embedding and slicing. After repairing the antigen with sodium citrate buffer, the MUC1 primary antibody (diluted 1:50, Abcam) was incubated at 4°C overnight, followed by incubating with second antibody (Maixin Biotech) for 30 min. The 3,3'-diaminobenzidine (DAB) staining kit (Maixin Biotech Co., Ltd.) was used for detection. Pictures were taken under $\times 200$ magnification in at least three random fields by using the BX53 + DP72 microscope (Olympus Corporation). Image-Pro Plus 6.0 image analysis software (Media Cybernetics, Inc.) was used for image analysis and evaluation.

2.11 | Xenograft tumors and bioluminescent imaging

All experiment procedures related to animals were performed according to the guidelines approved by the Institutional Animal Care and Use Committee of Guangdong Provincial Hospital of Chinese Medicine and the care and use of laboratory animals. A total of 32 female nude mice (6–8 weeks old) were purchased from Beijing Vital River Experimental Animal Co., Ltd. and maintained at the Animal Center of Guangdong Provincial Hospital of Chinese Medicine. HepG2-luc (5×10^6 /mice) was injected into the subaxillary skin of nude mice. The subcutaneous xenograft can be seen in about one week. Then mice were randomly divided into four groups ($n = 8$ /group): control group, SM group, SF group, and combination treatment group. SM and SF were intraperitoneally injected daily at the dose of 6 and 30 mg/kg for up to 25 days, respectively. During the experiment, the longest diameter and the shortest diameter of the xenograft tumors were measured using vernier caliper every 5 days. Mice were anesthetized by inhalation of 2% isoflurane for bioluminescence imaging (BLI). The substrate D-fluorescein (obtained from

Caliper Life Sciences) was injected into the abdominal cavity of the mice at a dose of 150 mg/kg. BLI signal strength was determined by the IVIS-200 imaging system (Xenogen/Caliper). Tumor volume was calculated using the ellipsoid volume formula: $\text{volume} = (\text{width}^2 \times \text{length})/2$. Quantification of bioluminescence was expressed as photons/sec. At the end of experiments, all mice were killed on day 25 according to the experimental animal care and use guidelines. Xenografted tumors were isolated and preserved. The expression of MUC1 protein was measured by WB, and qRT-PCR analysis was performed to determine the expressions of HOTTIP, TUG1, and miR-4726-5p.

2.12 | Statistical analysis

All in vitro experiments were performed at least three times. Statistical analysis was carried out using GraphPad Prism version 5.04 for Windows (GraphPad Software). All data are expressed as mean \pm SD. Pairwise comparisons were done by paired two-tailed *t*-test, Mann-Whitney test, or Fisher exact test. The data in most graphs are presented relative to the control. *p*-values < 0.05 were considered significant.

3 | RESULTS

3.1 | SM inhibited the tumor progression and enhanced the antitumor effect of SF on HCC

We demonstrated that SM inhibited the cell viability of human HepG2 and Huh-7 cells (Figure 1A). Moreover, cell proliferation was significantly reduced by SM described as percentage of EDU-positive cells, compared to the control group (Figure 1B). More importantly, the combination of SM and SF, a molecularly-targeted medicine that works on the vascular endothelial growth factor receptors,²⁷ had a synergistic inhibition on cell viability of HepG2 and Huh-7 cells in dose and time-dependent manner (Figure 1C).

3.2 | MUC1 mediated SM-induced inhibition of cell viability

Previously, we demonstrated an important role of MUC1 in growth of castration-resistant prostate cancer and non-small cell lung cancer.²⁸⁻³¹ However, the role of MUC1 in the tumorigenesis and development of HCC is still unclear. Herein, our results revealed that SM reduced the expression of MUC1 protein and mRNA in HepG2 and Huh-7 cells (Figure 2A,B). In addition, SM also significantly inactivated the MUC1 promoter activity (Figure 2C). More importantly, the combination of SM and SF had a synergistic effect on MUC1 protein expression (Figure 2D).

To confirm the role of MUC1 in SM-inhibited cell viability, MUC1 overexpression vectors were transfected into HepG2 and Huh-7 cells, MTT assay was used to detect the cell viability. The results showed that overexpression of MUC1 partially neutralized the effects of SM on cell viability (Figure 2E).

3.3 | MiR-4726-5p directly target to MUC1 and downregulated the expression of MUC1 protein

To further validate the role of MUC1 and interaction with other genes, miRNAs targeted to MUC1 were predicted by bioinformatics prediction databases, such as TargetScan, MiRWalk, and MiRBase. We found that classical binding sites in 3'-UTR region of MUC1 exist for several miRNAs, such as miR-4726-5p, miR-628-5p, miR-490-3p, miR-4778-3p, miR-194-3p, miR-328-3p, miR-143-3p, and miR-145-5p. The binding site for miR-4726-5p was evaluated with a context score percentile of 98, showing the highest degree of confidence (Figure 3A). Therefore, we focused on the miR-4726-5p for the subsequent study.

To identify the interaction between MUC1 and miR-4726-5p, HepG2 and Huh-7 cells were treated with miR-4726-5p mimics for 24 h. The results showed that miR-4726-5p mimics significantly reduced MUC1 protein expression in HepG2 and Huh-7 cells (Figure 3B). qRT-PCR results showed that the level of miR-4726-5p was significantly increased in cells transfected with miR-4726-5p mimics (Figure 3C).

Moreover, we generated a 3'-UTR cDNA fragment of MUC1 containing the wild-type and mutated miR-4726-5p binding sites (Figure 3D). Dual-luciferase reporter assay suggested that miR4726-5p mimics dramatically reduced the luciferase activity of wild-type 3'-UTR cDNA fragment of MUC1 compared with the mutated 3'-UTR or NC/scrambled mimics (Figure 3E). Taken together, these results suggested that miR-4726-5p may directly regulate MUC1 protein expression.

3.4 | SM upregulated the expression of miR-4726-5p in HCC cells

Next, we further researched the expression of 4726-5p in HCC and the interaction between SM and miR-4726-5p. Our results found that transcript abundance of miR-4726-5p in HepG2 and Huh-7 cells were lower compared with hepatic stellate cells (LX2) (Figure 4A). Moreover, SM significantly increased miR-4726-5p expression in HepG2 and Huh-7 cells as determined by qRT-PCR and RNA FISH analysis (Figure 4B,C). Moreover, the combination of SM and SF showed a significant synergy on activation of miR-4726-5p (Figure 4D). Furthermore, miR-4726-5p mimics significantly inhibited the growth of HepG2 and Huh-7 cells as compared with the control group (Figure 4E). These results suggested that miR-4726-5p may mediate the SM-induced growth inhibition of HCC cells.

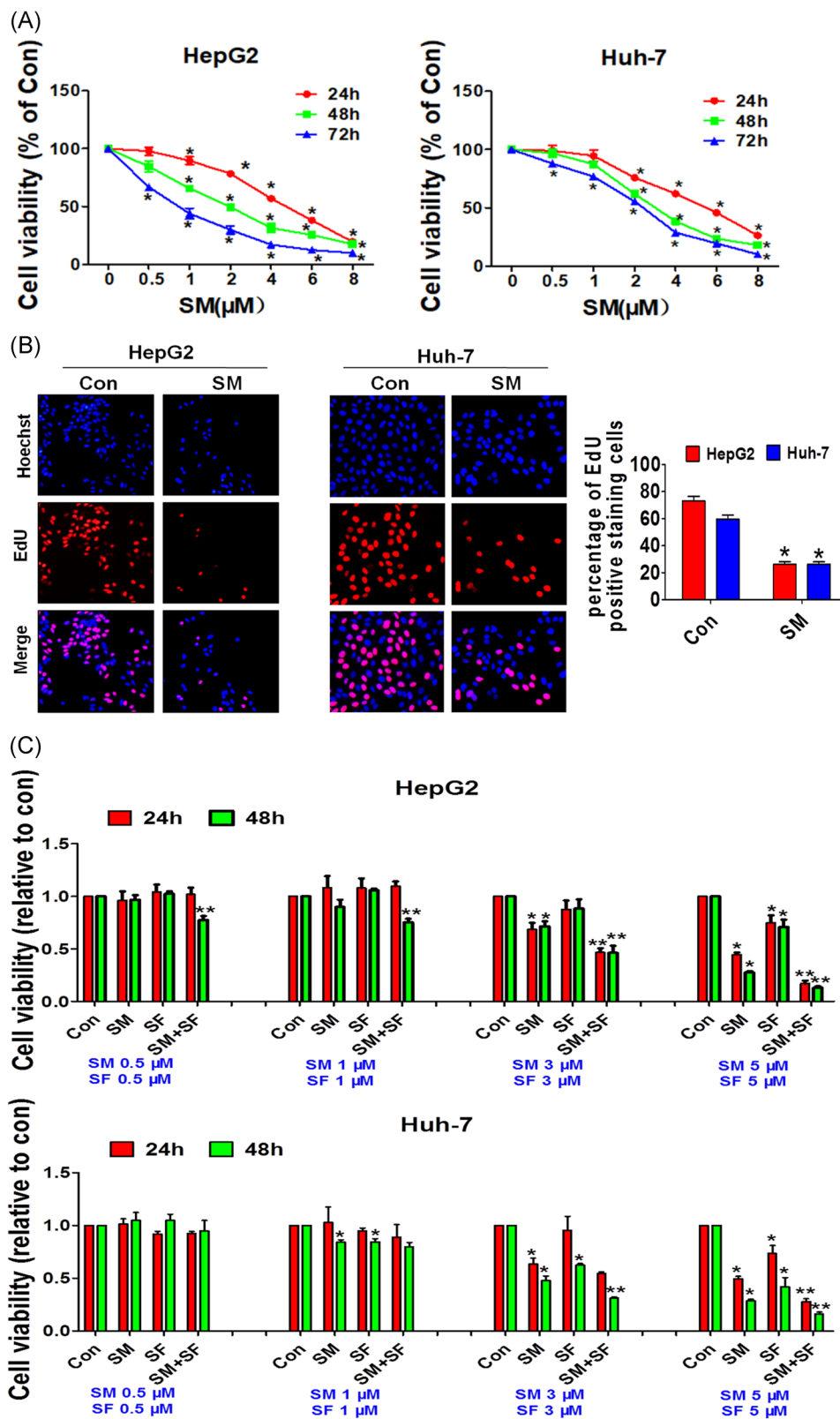


FIGURE 1 Solamargine (SM) inhibited cell viability and proliferation of HepG2 and Huh-7 cells. (A) HepG2 and Huh-7 cells were treated with indicated concentrations of SM (0, 0.5, 1, 2, 4, 6, 8 μM) for up to 72 h. 3-(4,5-dimethylthiazol-2-yl)-2,5-diphenyltetrazolium bromide (MTT) assay was performed to measure the cell viability. (B) HepG2 and Huh-7 cells were stimulated with SM (5 μM) for 24 h, followed by measuring the cell proliferation by using EDU assay as described in Section 2. (C) HepG2 and Huh-7 cells were treated with combination of SM and sorafenib for up to 48 h, followed by detecting the cell viability by MTT assays. *Significant difference from the control group ($p < 0.05$). **Significant difference from the SM or sorafenib (SF) alone ($p < 0.05$) [Color figure can be viewed at wileyonlinelibrary.com]

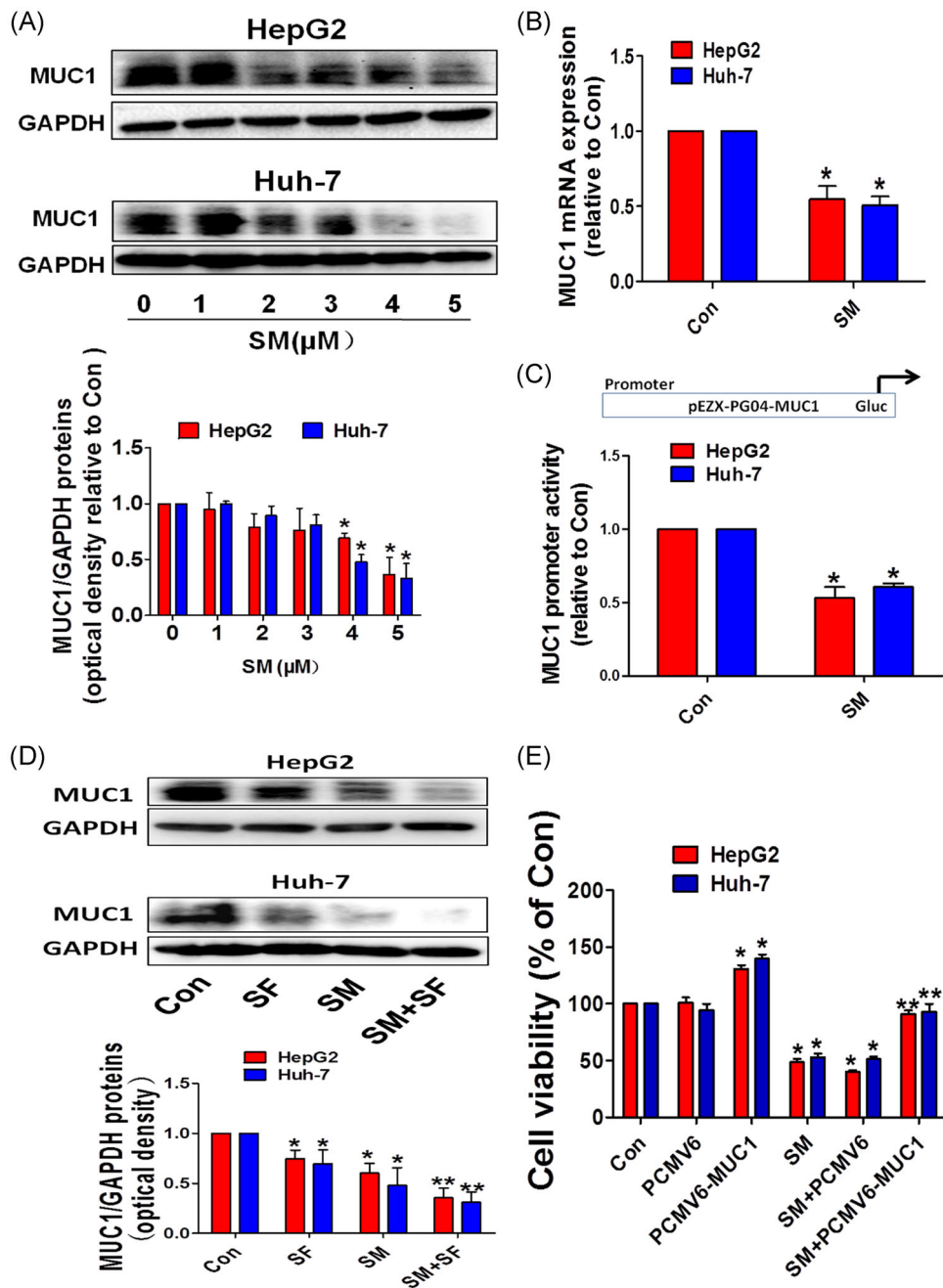
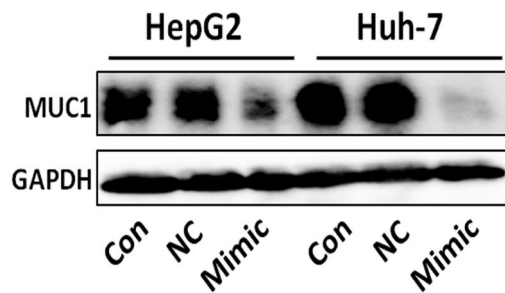


FIGURE 2 MUC1 mediated solamargine (SM)-induced inhibition of cell viability. (A) HepG2 and Huh-7 cells were stimulated with indicated doses of SM for 24 h, followed by detecting MUC1 protein expression by using Western blot analysis as described in the Section 2. (B) HepG2 and Huh-7 cells were treated with SM (5 μ M) for 24 h, then the expression of MUC1 mRNA was measured by real-time quantitative PCR analysis. (C) HepG2 and Huh-7 cells were transfected with MUC1 promoter plasmids or negative control (NC) for 24 h, then treated with SM (5 μ M) for an additional 24 h, dual-luciferase reporter assay was performed to measure the MUC1 promoter activity. (D) HepG2 and Huh-7 cells were treated with the combination of SM (5 μ M) and sorafenib (SF; 5 μ M) for 24 h, and then Western blot analysis was used to determine the expression of MUC1 protein. (E) HepG2 and Huh-7 cells were transfected with MUC1 overexpression or NC plasmids for 24 h before exposure of the cells to SM (5 μ M) for an additional 24 h, followed by measuring the cell viability by using 3-(4,5-dimethylthiazol-2-yl)-2,5-diphenyltetrazolium bromide assay as described in Section 2. Values and bar graphs are presented as the mean \pm SD of three independent experiments performed. *Significant difference from the NC group ($p < 0.05$). **Significant difference from the SM alone ($p < 0.05$) [Color figure can be viewed at wileyonlinelibrary.com]

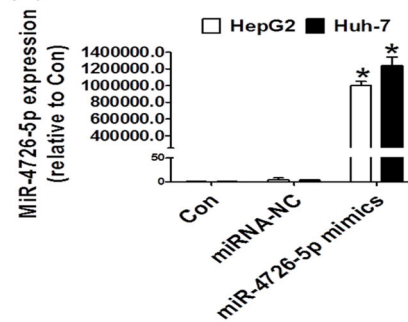
(A)

	Predicted consequential pairing of target region (top) and miRNA (bottom)	Site type	Context++ score	Context++ score percentile	Weighted context++ score
Position 416-423 of MUC1 3' UTR	5' ... GGGCUCGCCAGGAGGA-CUGGCCCA... 3' ... GGGCUCGCCAGGAGGA-CUGGCCCA... 	8mer	-0.48	98	-0.47
Position 90-96 of MUC1 3' UTR	5' ... GGUAGAGAAAGAAAGUCACAGCAG... 3' ... GGUAGAGAAAGAAAGUCACAGCAG... 	7mer-m8	-0.30	97	-0.30
Position 99-105 of MUC1 3' UTR	5' ... AGAAGUGDCAGCAGACAGGUUU... 3' ... AGAAGUGDCAGCAGACAGGUUU... 	7mer-m8	-0.24	96	-0.24
Position 82-88 of MUC1 3' UTR	5' ... GUUUCAGGUAGAAAGAAAGU... 3' ... GUUUCAGGUAGAAAGAAAGU... 	7mer-m8	-0.24	95	-0.24
Position 476-482 of MUC1 3' UTR	5' ... AAUAAAACGUGUCUCCACUC... 3' ... AAUAAAACGUGUCUCCACUC... 	7mer-m8	-0.25	95	-0.25
Position 240-246 of MUC1 3' UTR	5' ... CCACUCAGUUCUCAGGCCAG... 3' ... CCACUCAGUUCUCAGGCCAG... 	7mer-m8	-0.23	91	-0.23
Position 17-23 of MUC1 3' UTR	5' ... CCUCUGUCCCUAAUACUCC... 3' ... CCUCUGUCCCUAAUACUCC... 	7mer-m8	-0.17	90	-0.17
Position 451-457 of MUC1 3' UTR	5' ... ATAGCGGGAUCCUG----AACTGGAC... 3' ... ATAGCGGGAUCCUG----AACTGGAC... 	7mer-m8	-0.13	87	-0.13

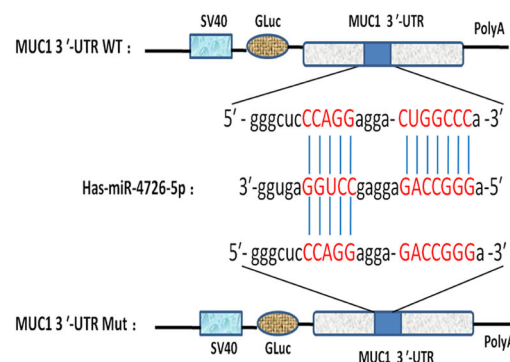
(B)



(C)



(D)



(E)

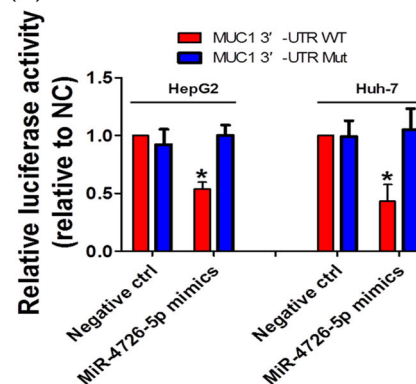


FIGURE 3 MUC1 acted as a direct target of miR-4726-5p. (A) The screen of microRNAs (miRNAs) targeting MUC1. (B) HepG2 and Huh-7 cells were transfected with miR-4726-5p mimics or negative control (NC) for 24 h, followed by measuring the expression of MUC1 protein by Western blot analysis as described in Section 2. (C) Quantification of miR-4726-5p was shown after transfecting miR-4726-5p mimics or NC for 24 h. (D) The binding site of miR-4726-5p and MUC1 was showed, and the dual-luciferase reporter vectors containing wild-type and mutant MUC1 mRNA 3'-UTR sequences were constructed. (E) HepG2 and Huh-7 cells were transfected with the pZX-MT05-Luc-MUC1-WT or pZX-MT05-Luc-MUC1-Mut vectors for 24 h, followed by treating with the miR-4726-5p mimics (100 nmol/L) or miRNA-NC for an additional 48 h. Afterwards, Secrete-Pair™ Dual Luminescence Assay Kit was used to detect the luciferase activity as described in Section 2. Values and bar graphs are presented as the mean \pm SD of three independent experiments performed. *Significant difference from the NC group ($p < 0.05$). **Significant difference from the solamargine alone ($p < 0.05$) [Color figure can be viewed at wileyonlinelibrary.com]

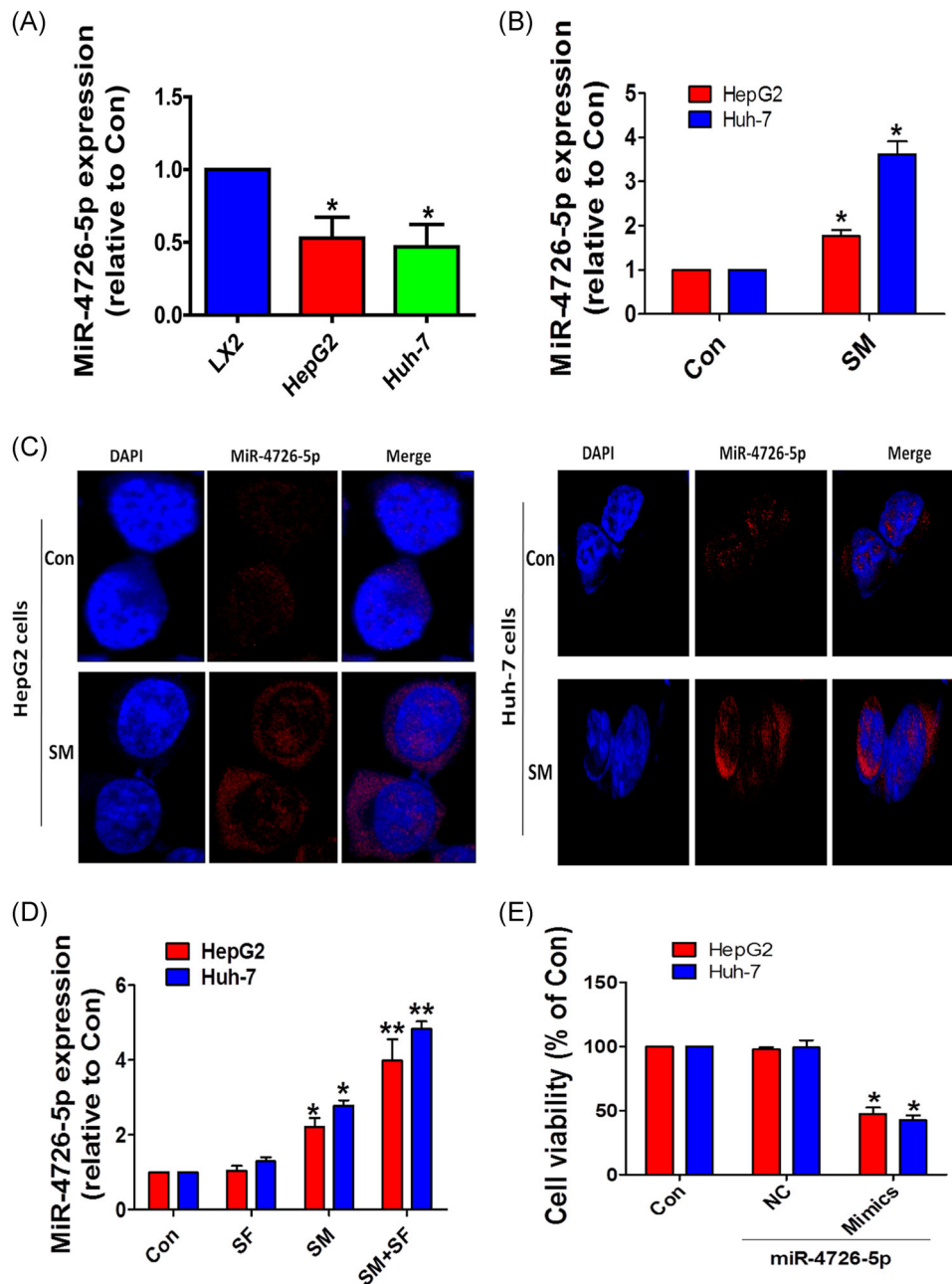


FIGURE 4 Solamargine (SM) increased the expression of miR-4726-5p in hepatocellular carcinoma cells. (A) Total RNA was isolated from HepG2, Huh-7, and LX2 (hepatic stellate cell line) cells and processed for determining the expression level of miR-4726-5p by using real-time quantitative PCR (qRT-PCR) analysis. (B) HepG2 and Huh-7 cells were treated with SM (5 μ M) for 24 h, followed by detecting miR-4726-5p by qRT-PCR analysis as described in Section 2. (C) HepG2 and Huh-7 cells were incubated with SM (5 μ M) for 24 h, situ expression level of miR-4726-5p were measured by using RNA fluorescence in situ hybridization assay as described in Section 2. (D) HepG2 and Huh-7 cells were treated with SM (5 μ M) and sorafenib (SF; 5 μ M) for up to 24 h, total RNA was isolated and qRT-PCR analysis was used to determine the expression of miR-4726-5p. (E) HepG2 and Huh-7 cells were transfected with miR-4726-5p mimics or negative control (NC) for 48 h, 3-(4,5-dimethylthiazol-2-yl)-2,5-diphenyltetrazolium bromide assay was performed to measure the cell viability. *Significant difference from the control group ($p < 0.05$). **Significant difference from the SM or SF alone ($p < 0.05$) [Color figure can be viewed at wileyonlinelibrary.com]

3.5 | HOTTIP and TUG1 acted as the sponge of miR-4726-5p

By utilizing bioinformatics prediction databases, we found that miR-4726-5p has a classical and conservative binding site in the region of

HOTTIP or TUG1 respectively (Figure 5A). Subsequently, we generated a cDNA fragment of HOTTIP or TUG1 containing the wild-type and mutated binding sites of miR-4726-5p (Figure 5A).

To determine the interaction between HOTTIP or TUG1 and miR-4726-5p in mediating the effect of SM. We transfected HOTTIP

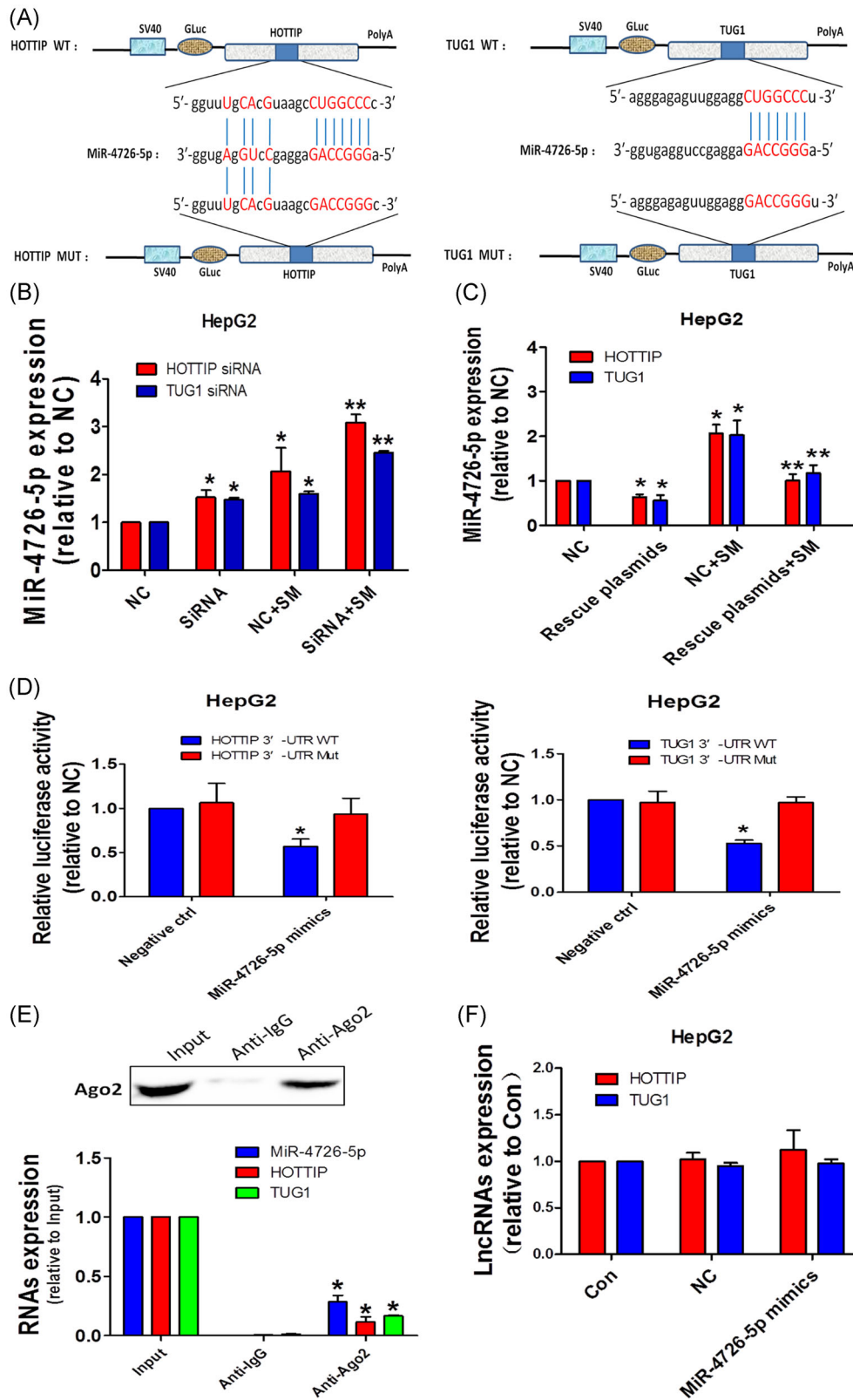


FIGURE 5 (See caption on next page)

and TUG1 siRNA into HepG2 cells, the results showed that silencing of HOTTIP or TUG1 dramatically enhanced the effect of SM-induced expression of miR-4726-5p (Figure 5B). Conversely, overexpression of HOTTIP and TUG1 suppressed miR-4726-5p expression and reversed the effect of SM-induced expression of miR-4726-5p in HepG2 cells (Figure 5C). HOTTIP and TUG1 rescue plasmids could significantly increase the expression of HOTTIP and TUG1 (Figure S1).

Then, dual-luciferase reporter assay was performed to measure the luciferase activities, the results showed that miR-4726-5p mimics significantly decreased the luciferase activities in HepG2 cells transfected with wild-type cDNA fragment of HOTTIP or TUG1, compared to NC group (Figure 5D).

Furthermore, RIP assay revealed that HOTTIP, TUG1, and miR-4726-5p were enriched in the Ago2-containing beads and were higher compared with the IgG group, which suggested that there were physical binding between HOTTIP, TUG1, and miR-4726-5p in HepG2 cells (Figure 5E). However, miR-4726-5p mimics have no significant effect on HOTTIP and TUG1 expression (Figure 5F). Taken together, these results suggested that the physical interaction between HOTTIP or TUG1 and miR-4726-5p may also play an additional role in mediating the anticancer effect of SM.

3.6 | HOTTIP and TUG1 were decreased by SM and mediated the progression of HCC

Recent studies have demonstrated the important role of lncRNAs such as HOTTIP and TUG1 in the progression of cancers.^{12,32} Herein, our results revealed that SM significantly reduced the expression of HOTTIP and TUG1 in HepG2 and Huh-7 cells (Figure 6A). Silencing of HOTTIP and TUG1 significantly inhibited the cell viability of HepG2 and Huh-7 cells as determined by MTT assays (Figure 6B). Conversely, overexpression of HOTTIP and TUG1 promoted cell viability and reversed the effect of SM-inhibited cell viability of HepG2 and Huh-7 cells (Figure 6C). QPCR results showed that HOTTIP and TUG1 rescue plasmids successfully caused HOTTIP and TUG1 overexpression in HepG2 and Huh-7 cells (Figure S2). Interestingly, silence of TUG1 dramatically decreased the expression of HOTTIP, while HOTTIP knockdown had no significant effect on

TUG1 expression in HepG2 and Huh-7 cells (Figure 6D,E). Taken together, our results demonstrated that HOTTIP and TUG1 may be the important targets of SM and involved in the SM-mediated inhibition of HCC cells.

3.7 | SM combined with SF synergistically inhibited tumor growth by regulating the expressions of HOTTIP, TUG1, miR-4726-5p, and MUC1 in vivo

To validate the results in vitro, we constructed the xenografts model in nude mice to test the antitumor effect of SM and SF. Luciferase-expressing HepG2 cells (HepG2-Luc) were injected subcutaneously in nude mice followed by intraperitoneal injection of D-luciferin. Mice bearing xenografted tumors were treated with saline, SM, SF, and combination of SM and SF via intraperitoneal injection for up to 25 days. We found that compared to the control group, SM significantly inhibited tumor growth and luciferase activity as measured by the Xenogen IVIS200 System (Figure 7A,B). More importantly, a further growth-inhibitory effect was observed in the combination treatment group (Figure 7A,B). In addition, we found a reduction of the tumor weight and volume in the SF or SM alone group as compared to that in the control group (Figure 7C,D). The combination treatment brought a further inhibitory effect on the tumor weight and volume (Figure 7C,D). Furthermore, consistent with the in vitro results, the reduced expression of MUC1 protein, HOTTIP, and TUG1 whereas increased miR-4726-5p expression was observed in fresh tumors harvested from nude mice (Figure 7E-H), and the combination of SM and SF showed a synergy effects on the above targets (Figure 7E-H). Taken together, these results indicated that both in vitro and in vivo results showed similar effects of SM and SF on HCC growth and relevant targets expression.

4 | DISCUSSION

The comparison of the results in vivo and in vitro further confirmed that SM had a significant growth inhibition effect on HCC. Mechanically, SM inhibited cell growth through the interaction and

FIGURE 5 Solamargine (SM) elevated miR-4726-5p expression through downregulation of HOTTIP and TUG1. (A) Bioinformatics prediction databases were used to predict the binding site between miR-4726-5p and HOTTIP or TUG1 respectively. The dual-luciferase reporter constructs containing a wild-type and mutant HOTTIP and TUG1 sequences were shown here. (B and C) HepG2 cells were transfected with HOTTIP or TUG1 siRNAs/plasmids and negative control (NC) for 24 h, then treated with SM for an additional 24 h, real-time quantitative PCR (qRT-PCR) analysis was performed to measure the expression of miR-4726-5p. (D) HepG2 cells were transfected with the pEZX-MT05-Luc-HOTTIP (or TUG1)-WT or pEZX-MT05-Luc-HOTTIP (or TUG1)-Mut vectors for 24 h, and then treated with the miR-4726-5p mimics (100 nmol/L) or microRNA (miRNA)-NC for an additional 48 h. Afterwards, SecretE-Pair™ Dual Luminescence Assay Kit was used to detect the luciferase activity. (E) Cell lysates from HepG2 cells were incubated with Ago2 antibody-coated magnetic beads. Precipitates were detected for Ago2 protein by using Western blot analysis as described in Section 2, preimmune IgG and input from cell extracts were used as controls (upper panel). qRT-PCR was performed to determine the expression levels of HOTTIP, TUG1, and miR-4726-5p (lower panel). (F) HepG2 cells were transfected with miR-4726-5p mimics for 48 h, qRT-PCR analysis was performed to determine the expression of HOTTIP and TUG1. Values and bar graphs are presented as the mean ± SD of three independent experiments performed. *Significant difference from the NC group or IgG group ($p < 0.05$). **Significant difference from the SM alone ($p < 0.05$) [Color figure can be viewed at wileyonlinelibrary.com]

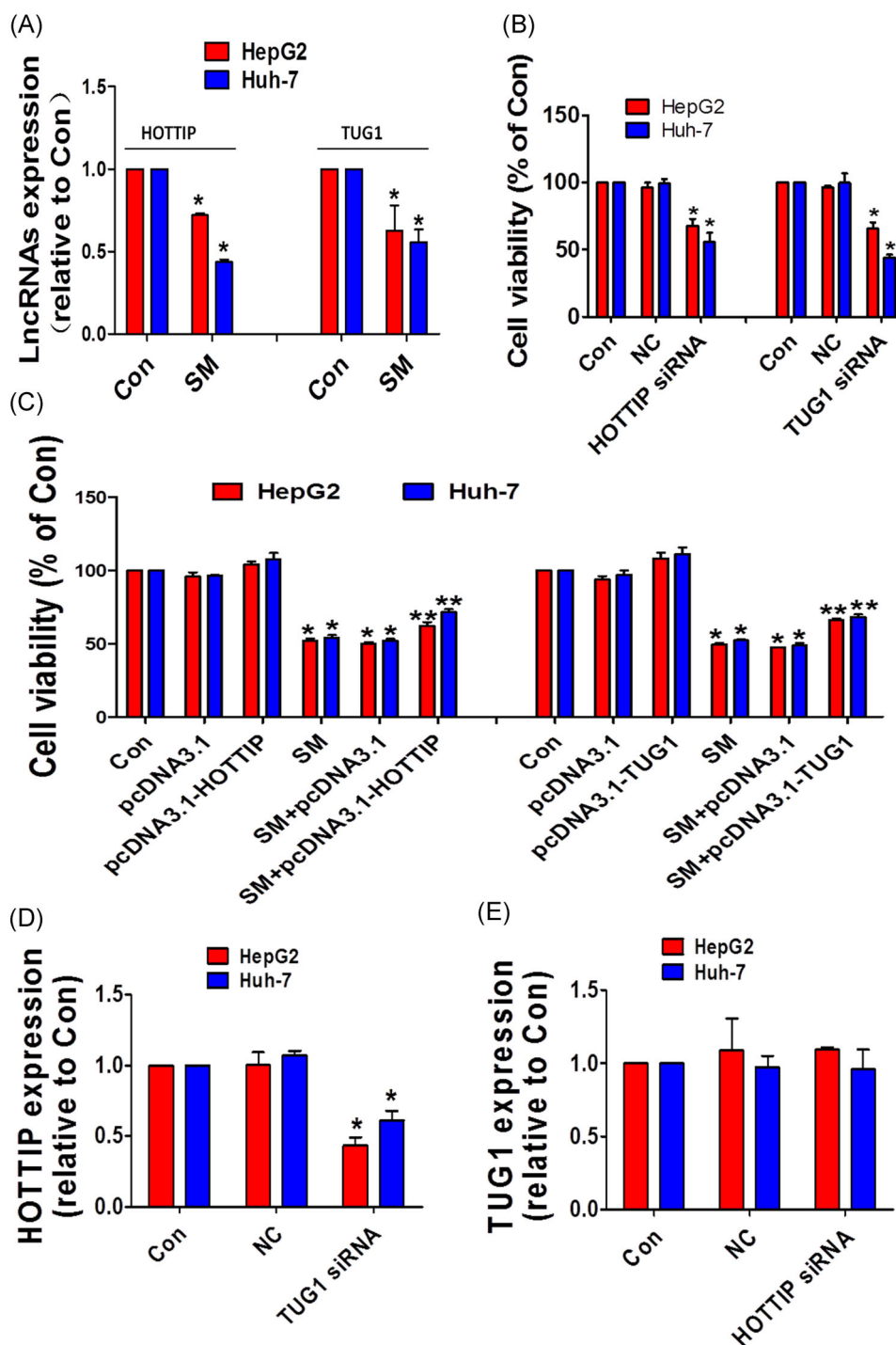


FIGURE 6 Solamargine (SM) inhibited cell viability of hepatocellular carcinoma via suppression of HOTTIP and TUG1. (A) HepG2 and Huh-7 cells were treated with SM (5 μ M) for 24 h, followed by determination of HOTTIP and TUG1 expression by using real-time quantitative PCR analysis as described in Section 2. (B and C) HepG2 and Huh-7 cells were transfected with HOTTIP and TUG1 siRNA/overexpression plasmids for 24 h, and then treated with/without SM for additional 24 h, 3-(4,5-dimethylthiazol-2-yl)-2,5-diphenyltetrazolium bromide assay was performed to detect the cell viability. (D and E) HepG2 and Huh-7 cells were transfected with HOTTIP and TUG1 siRNA for 24 h, followed by determining the expression of TUG1 and HOTTIP, respectively. *Significant difference from the control group ($p < 0.05$). **Significant difference from the SM alone. NC, negative control ($p < 0.05$) [Color figure can be viewed at wileyonlinelibrary.com]

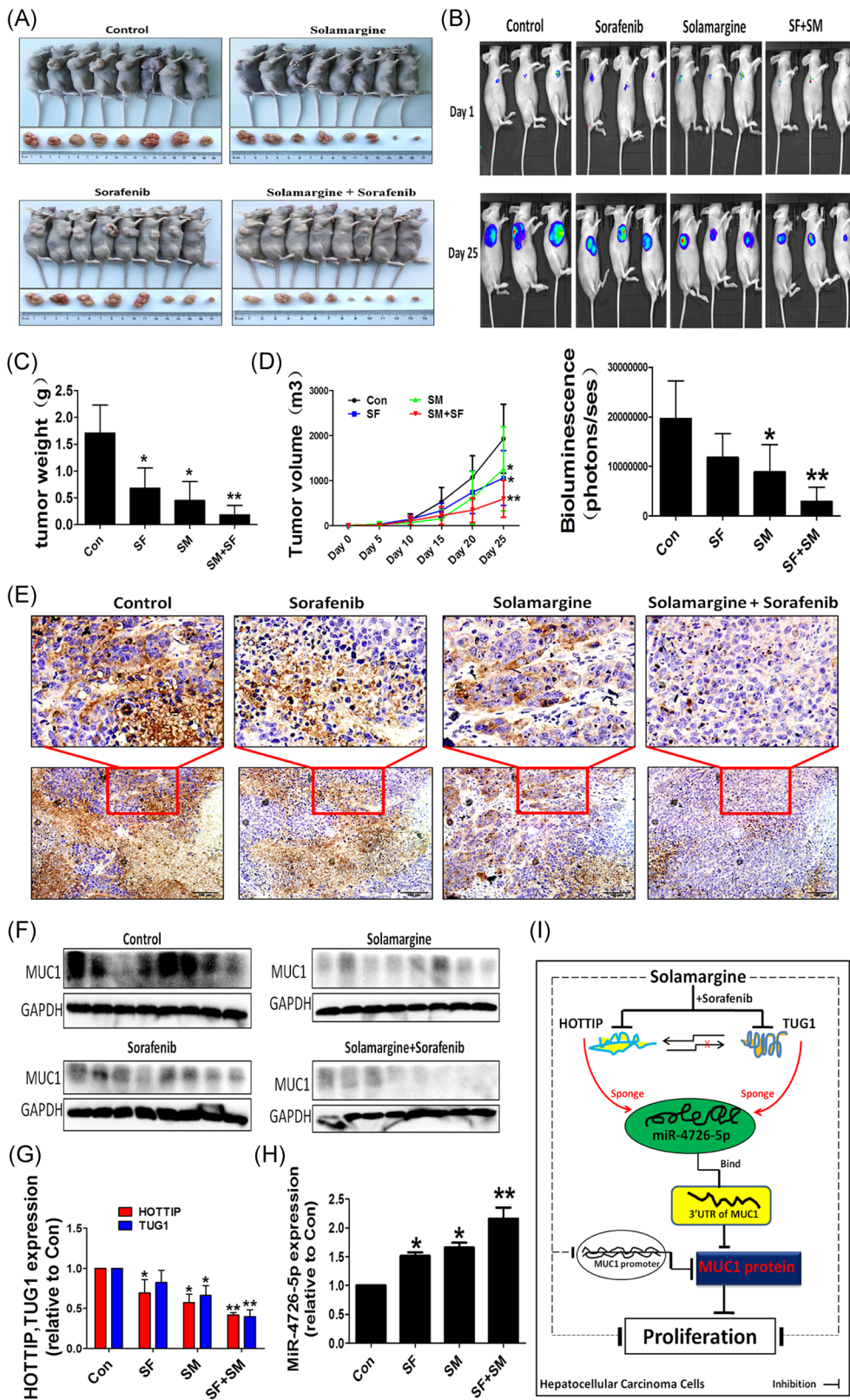


FIGURE 7 (See caption on next page)

feedback regulatory axis between HOTTIP, TUG1, miR-4726-5p, and MUC1. The dose of SM is based on our previous report and another study that showed a significant inhibitory effect on tumor growth without significant toxicity.

Recent study showed that high HOTTIP expression was closely associated with poor overall survival, lymph node metastasis, distant metastasis, and tumor stage, suggesting that high HOTTIP expression could be a potential biomarker for poor prognosis of cancer.³³ For example, HOTTIP promoted the secretion of IL-6, thereby upregulating the expression of PD-L1 in neutrophils, and finally accelerating the immune escape of ovarian cancer.³⁴ Moreover, HOTTIP silencing significantly inhibited the proliferation, cell cycle, migration, and invasion of nasopharyngeal carcinoma cells through acting as a sponge for miR-4301.³⁵ Similarly, studies have reported that TUG1 involved in the tumorigenesis and development of human cancer, including proliferation, apoptosis, migration, metastasis, drug-resistance, and so on.^{36–40} For instance, TUG1 was highly expressed in cholangiocarcinoma cells and promoted the cell proliferation and invasion but inhibited the cell apoptosis through acting as a sponge of miR-29a.⁴¹ In this study, we first validated that HOTTIP and TUG1 both are important target genes of SM in HCC cells. We found that SM could simultaneously down-regulate the expression of HOTTIP and TUG1 in HepG2 and Huh-7 cells, and an interaction between HOTTIP and TUG1 was confirmed. Moreover, there is a classical and conservative binding site for miR-4726-5p in the region of HOTTIP and TUG1 sequence, which co-contributed to the inhibitory effect of SM on the growth of HCC.

Importantly, our findings confirmed the role of MUC1 in SM-mediated growth inhibition of HCC. Aberrantly elevated MUC1 expression positively correlates with growth, progression, drug resistance, immune modulation, metastasis, and poor prognosis through regulation of several important downstream molecules or targets.^{26,42–45} Consistent with this, our findings suggested that downregulation of MUC1 was required to mediate SM-suppressed the growth of HCC. We found that elevating MUC1 expression significantly reversed the growth inhibitory effect of SM on HCC cells. More importantly, the combination of SM and SF had a significant synergy effect on MUC1 protein expression. HOTTIP, TUG1, and miR-4726-5p acted as upstream regulators to mediate the regulation of SM on MUC1 protein. However, whether changes of MUC1 expression lead to feedback regulation of the above genes requires further experimental validation.

In addition to HCC, our previous study had demonstrated that MUC1 mediated the growth inhibition of androgen nondependent prostate cancer cells by the herbal monomer curcumin through interaction with SAPK/JNK and MEK/ERK1/2 and NF- κ B/p6530. MUC1 mediated the regulation of lncRNA-ROR/miR-145 on invasion and migration of TNBC cells, and enhanced the aggressiveness of cancer cells by inducing EMT.⁴⁶ Moreover, MUC1 was associated with methylation of TFF2, a member of secreted peptides, which is also expressed in gastric mucosa and triggers cell migration signaling to promote epithelial repair and involve in GC development.⁴⁷ Therefore, MUC1 played a key role in the development of many human cancers including HCC.

Collectively, our results showed that SM inhibited growth of HCC cells through inactivation of HOTTIP and TUG1, followed by upregulation of miR-4726-5p, this ultimately inhibited the expression of MUC1 protein. As expected, our *in vivo* data were consistent with the *in vitro* results, confirming that SM significantly inhibited the growth of HCC and enhanced the anticancer effect of SF by regulating the HOTTIP-TUG1/miR-4726-5p/MUC1 signaling pathway. The present results improve our understanding of the underlying mechanisms involved in the anticancer effect of SM and further confirm a potential treatment for human HCC. However, the inter-regulatory relationships among the above genes are difficult to be accurately and effectively verified *in vivo*, so more reasonable experiments need to be designed to confirm their inter-regulatory networks *in vivo* in the future.

5 | CONCLUSIONS

Our results showed that SM significantly inhibited the expression of MUC1 protein by upregulating the expression of miR-4726-5p, which was coregulated by lncRNA HOTTIP and TUG1. This complex interaction and modulation of the feedback axis contribute to the overall anticancer effect of SM and SF *in vivo* and *in vitro* (Figure 7I). These findings improve our understanding of the potential mechanisms by which SM enhances the anticancer effects of SF and provide new molecular targets for the treatment of HCC.

ACKNOWLEDGMENTS

This study was supported by the grants from the Scientific Research Project in Universities of Guangdong Provincial Department of

FIGURE 7 Antitumor efficacy of solamargine (SM) combined with sorafenib (SF) *in vivo*. (A and B) Mice ($n = 8$ /group) were divided to four groups (Con [saline], SF [30 mg/kg], SM [6 mg/kg], and SM plus SF). The tumor growth was monitored by injecting luciferin followed by measuring bioluminescence signals at the initial and end of the experiments. (C and D) The xenografts were harvested on Day 25, the tumor weight and tumor volume were measured. (E and H) The xenograft tumors were isolated and processed for detecting MUC1, HOTTIP, TUG1, and miR-4726-5p by using IHC, Western blot, and real-time quantitative PCR analysis, respectively. (I) The diagram showed that SM inhibits the cell growth of hepatocellular carcinoma (HCC) through inactivation of lncRNA HOTTIP and TUG1, followed by increasing the expression of miR-4726-5p, this ultimately suppresses the promoter activity and protein expression of MUC1. This complex interaction and feedback regulatory axis contribute to the synergy inhibition effect of combination of SM and SF in HCC. *Significant difference as compared to the untreated control group ($p < 0.05$). **Significant difference from the SM or SF alone ($p < 0.05$) [Color figure can be viewed at wileyonlinelibrary.com]

Education (2020KTSCX029); the Chinese Medicine Science and Technology Research Project of Guangdong Provincial Hospital of Chinese Medicine (YN2019MJ09, YN2019QJ06); the Guangdong Provincial Key Laboratory of Clinical Research on Traditional Chinese Medicine Syndrome (ZH2020KF03); the State Key Laboratory of Dampness Syndrome of Chinese Medicine Special Fund (SZ2021ZZ29) and postgraduate research innovation project of Guangzhou University of Chinese Medicine (A1-2606-21-429-001Z53).

CONFLICT OF INTERESTS

The authors declare that there are no conflict of interests.

AUTHOR CONTRIBUTIONS

Qing Tang, Xiaojuan Li, and Yun Chen performed most of the experiments and drafted the manuscript. Shunqing Long, Yaya Yu, and Honghao Sheng performed some of the experiments. Sumei Wang edited the manuscript and provided some crucial suggestions. Ling Han provided funding and administrative support. Wanyin Wu contributed to the conception and designed the present project. All authors listed approved the publication of this article.

DATA AVAILABILITY STATEMENT

The data that support the findings of this study are available from the corresponding author upon reasonable request. All data generated and analyzed during the current study are included in this article and available from the corresponding author on reasonable request.

ORCID

Qing Tang  <https://orcid.org/0000-0002-2128-4810>

REFERENCES

- Kim DW, Talati C, Kim R. Hepatocellular carcinoma (HCC): beyond sorafenib-chemotherapy. *J Gastrointest Oncol*. 2017;8(2):256-265.
- Couri T, Pillai A. Goals and targets for personalized therapy for HCC. *Hepatol Int*. 2019;13(2):125-137.
- Han Q, Zhao H, Jiang Y, Yin C, Zhang J. HCC-derived exosomes: critical player and target for cancer immune escape. *Cells*. 2019;8(6):558.
- Tang Q, Zheng F, Liu Z, et al. Novel reciprocal interaction of lncRNA HOTAIR and miR-214-3p contribute to the solamargine-inhibited PDPK1 gene expression in human lung cancer. *J Cell Mol Med*. 2019;23(11):7749-7761.
- Wu J, Tang X, Ma C, Shi Y, Wu W, Hann SS. The regulation and interaction of colon cancer-associated transcript-1 and miR7-5p contribute to the inhibition of SP1 expression by solamargine in human nasopharyngeal carcinoma cells. *Phytother Res*. 2020;34(1):201-213.
- Fu R, Wang X, Hu Y, et al. Solamargine inhibits gastric cancer progression by regulating the expression of lncNEAT1_2 via the MAPK signaling pathway. *Int J Oncol*. 2019;54(5):1545-1554.
- Al Sinani SS, Eltayeb EA, Coomber BL, Adham SA. Solamargine triggers cellular necrosis selectively in different types of human melanoma cancer cells through extrinsic lysosomal mitochondrial death pathway. *Cancer Cell Int*. 2016;16:11.
- Kalalinia F, Karimi-Sani I. Anticancer properties of solamargine: a systematic review. *Phytother Res*. 2017;31(6):858-870.
- Xie X, Zhang X, Chen J, et al. Fe₃O₄-solamargine induces apoptosis and inhibits metastasis of pancreatic cancer cells. *Int J Oncol*. 2019;54(3):905-915.
- Wang L, Cho KB, Li Y, Tao G, Xie Z, Guo B. Long noncoding RNA (lncRNA)-mediated competing endogenous RNA networks provide novel potential biomarkers and therapeutic targets for colorectal cancer. *Int J Mol Sci*. 2019;20(22):5758.
- Chen Z, He A, Wang D, Liu Y, Huang W. Long noncoding RNA HOTTIP as a novel predictor of lymph node metastasis and survival in human cancer: a systematic review and meta-analysis. *Oncotarget*. 2017;8(8):14126-14132.
- Zhou H, Sun L, Wan F. Molecular mechanisms of TUG1 in the proliferation, apoptosis, migration and invasion of cancer cells. *Oncol Lett*. 2019;18(5):4393-4402.
- Shen X, Hu X, Mao J, et al. The long noncoding RNA TUG1 is required for TGF- β /TWIST1/EMT-mediated metastasis in colorectal cancer cells. *Cell Death Dis*. 2020;11(1):65.
- Wang X, Peng J, Wang J, et al. Hepatitis C virus core impacts expression of miR122 and miR204 involved in carcinogenic progression via regulation of TGFBRAP1 and HOTTIP expression. *Oncotargets Ther*. 2018;11:1173-1182.
- Wu L, Yang Z, Zhang J, Xie H, Zhou L, Zheng S. Long noncoding RNA HOTTIP expression predicts tumor recurrence in hepatocellular carcinoma patients following liver transplantation. *Hepatobiliary Surg Nutr*. 2018;7(6):429-439.
- Zhao W, Jiang X, Yang S. lncRNA TUG1 promotes cell proliferation, migration, and invasion in hepatocellular carcinoma via regulating miR-29c-3p/COL1A1 axis. *Cancer Manag Res*. 2020;12:6837-6847.
- Refai NS, Louka ML, Halim HY, Montasser I. Long non-coding RNAs (CASC2 and TUG1) in hepatocellular carcinoma: clinical significance. *J Gene Med*. 2019;21(9):e3112.
- Mohyeldeen M, Ibrahim S, Shaker O, Helmy H. Serum expression and diagnostic potential of long non-coding RNAs NEAT1 and TUG1 in viral hepatitis C and viral hepatitis C-associated hepatocellular carcinoma. *Clin Biochem*. 2020;84:38-44.
- Lin YH, Wu MH, Huang YH, Yeh CT, Lin KH. TUG1 is a regulator of AFP and serves as prognostic marker in non-hepatitis B non-hepatitis C hepatocellular carcinoma. *Cells*. 2020;9(2):262.
- Iqbal MA, Arora S, Prakasam G, Calin GA, Syed MA. MicroRNA in lung cancer: role, mechanisms, pathways and therapeutic relevance. *Mol Aspects Med*. 2019;70:3-20.
- Fan Y, Xia X, Zhu Y, et al. Circular RNA expression profile in laryngeal squamous cell carcinoma revealed by microarray. *Cell Physiol Biochem*. 2018;50(1):342-352.
- Yadi W, Shurui C, Tong Z, Suxian C, Qing T, Dongning H. Bioinformatic analysis of peripheral blood miRNA of breast cancer patients in relation with anthracycline cardiotoxicity. *BMC Cardiovasc Disord*. 2020;20(1):43.
- Tayebi B, Abrishami F, Alizadeh S, et al. Modulation of microRNAs expression in hematopoietic stem cells treated with sodium butyrate in inducing fetal hemoglobin expression. *Artif Cells Nanomed Biotechnol*. 2017;45(1):146-156.
- Hu B, Xiao L, Wang C, et al. Circ_0022382 ameliorated intervertebral disc degeneration by regulating TGF- β ₃ expression through sponge adsorption of miR-4726-5p. *Bone*. 2021;154:116185.
- Wang XT, Kong FB, Mai W, Li L, Pang LM. MUC1 immunohistochemical expression as a prognostic factor in gastric cancer: meta-analysis. *Dis Markers*. 2016;2016:9421571.
- Bhatia R, Gautam SK, Cannon A, et al. Cancer-associated mucins: role in immune modulation and metastasis. *Cancer Metastasis Rev*. 2019;38(1-2):223-236.

27. Cabral LKD, Tiribelli C, Sukowati CHC. Sorafenib resistance in hepatocellular carcinoma: the relevance of genetic heterogeneity. *Cancers (Basel)*. 2020;12(6):1576.
28. Xiang S, Zou P, Wu J, et al. Crosstalk of NF- κ B/P65 and LncRNA HOTAIR-mediated repression of MUC1 expression contribute to synergistic inhibition of castration-resistant prostate cancer by polyphyllin 1-enzalutamide combination treatment. *Cell Physiol Biochem*. 2018;47(2):759-773.
29. Xiang S, Zhang Q, Tang Q, et al. Activation of AMPK α mediates additive effects of solamargine and metformin on suppressing MUC1 expression in castration-resistant prostate cancer cells. *Sci Rep*. 2016;6:36721.
30. Li J, Xiang S, Zhang Q, et al. Combination of curcumin and bicalutamide enhanced the growth inhibition of androgen-independent prostate cancer cells through SAPK/JNK and MEK/ERK1/2-mediated targeting NF- κ B/p65 and MUC1-C. *J Exp Clin Cancer Res*. 2015;34(1):46.
31. Li L, Wang S, Zheng F, Wu W, Hann SS. Chinese herbal medicine Fuzheng Kang-Ai decoction sensitized the effect of gefitinib on inhibition of human lung cancer cells through inactivating PI3-K/Akt-mediated suppressing MUC1 expression. *J Ethnopharmacol*. 2016;194:918-929.
32. Ghafouri-Fard S, Dashti S, Taheri M. The HOTTIP (HOXA transcript at the distal tip) lncRNA: review of oncogenic roles in human. *Biomed Pharmacother*. 2020;127:110158.
33. Fan Y, Yan T, Chai Y, Jiang Y, Zhu X. Long noncoding RNA HOTTIP as an independent prognostic marker in cancer. *Clin Chim Acta*. 2018;482:224-230.
34. Shang A, Wang W, Gu C, et al. Long non-coding RNA HOTTIP enhances IL-6 expression to potentiate immune escape of ovarian cancer cells by upregulating the expression of PD-L1 in neutrophils. *J Exp Clin Cancer Res*. 2019;38(1):411.
35. Shen M, Li M, Liu J. Long noncoding RNA HOTTIP promotes nasopharyngeal cancer cell proliferation, migration, and invasion by inhibiting miR-4301. *Med Sci Monit*. 2019;25:778-785.
36. Li T, Chen Y, Zhang J, Liu S. LncRNA TUG1 promotes cells proliferation and inhibits cells apoptosis through regulating AURKA in epithelial ovarian cancer cells. *Medicine (Baltimore)*. 2018;97(36):e12131.
37. Gu L, Li Q, Liu H, Lu X, Zhu M. Long noncoding RNA TUG1 promotes autophagy-associated paclitaxel resistance by sponging miR-29b-3p in ovarian cancer cells. *Onco Targets Ther* 2020;13:2007-2019.
38. Wang X, Bai X, Yan Z, et al. The lncRNA TUG1 promotes cell growth and migration via the TUG1/miR-145-5p/TRPC6 pathway in colorectal cancer. *Biochem Cell Biol*. 2020;99(2):249-260.
39. Duan W, Nian L, Qiao J, Liu NN. LncRNA TUG1 aggravates the progression of cervical cancer by binding PUM2. *Eur Rev Med Pharmacol Sci*. 2019;23(19):8211-8218.
40. Shao H, Dong D, Shao F. Long non-coding RNA TUG1-mediated down-regulation of KLF4 contributes to metastasis and the epithelial-to-mesenchymal transition of colorectal cancer by miR-153-1. *Cancer Manag Res*. 2019;11:8699-8710.
41. Hao WY, Guo LW, Luo J, Shao GL, Zheng JP. LncRNA TUG1 promotes growth and metastasis of cholangiocarcinoma cells by inhibiting miR-29a. *Cancer Manag Res*. 2020;12:11103-11111.
42. Zong ZH, Du YP, Guan X, Chen S, Zhao Y. CircWHSC1 promotes ovarian cancer progression by regulating MUC1 and hTERT through sponging miR-145 and miR-1182. *J Exp Clin Cancer Res*. 2019;38(1):437.
43. Jing X, Liang H, Hao C, et al. Overexpression of MUC1 predicts poor prognosis in patients with breast cancer. *Oncol Rep*. 2019;41(2):801-810.
44. Farahmand L, Merikhan P, Jalili N, Darvishi B, Majidzadeh-A K. Significant role of MUC1 in development of resistance to currently existing anti-cancer therapeutic agents. *Curr Cancer Drug Targets*. 2018;18(8):737-748.
45. Yu B, You W, Chen G, Yu Y, Yang Q. MiR-140-5p inhibits cell proliferation and metastasis by regulating MUC1 via BCL2A1/MAPK pathway in triple negative breast cancer. *Cell Cycle*. 2019;18(20):2641-2650.
46. Ma J, Yang Y, Huo D, et al. LincRNA-RoR/miR-145 promote invasion and metastasis in triple-negative breast cancer via targeting MUC1. *Biochem Biophys Res Commun*. 2018;500(3):614-620.
47. Ge Y, Ma G, Liu H, et al. MUC1 is associated with TFF2 methylation in gastric cancer. *Clin Epigenetics*. 2020;12(1):37.

SUPPORTING INFORMATION

Additional supporting information may be found in the online version of the article at the publisher's website.

How to cite this article: Tang Q, Li X, Chen Y, et al. Solamargine inhibits the growth of hepatocellular carcinoma and enhances the anticancer effect of sorafenib by regulating HOTTIP-TUG1/miR-4726-5p/MUC1 pathway. *Molecular Carcinogenesis*. 2022;61:417-432. doi:10.1002/mc.23389